INDIAN JOURNAL OF SCIENCE AND TECHNOLOGY

ORIGINAL ARTICLE

Adaptive Rhea Optimization Enhanced CNN SVM Framework (ROC-SVM) for Precise MRI Based Brain Tumor Classification

S Shanmugapriya[1]*, P Rutravigneshwaran[2]

1 Research Scholar, Department of Computer Science, Karpagam Academy of Higher Education, Coimbatore, Tamil Nadu, India and Assistant Professor, Department of Computer Science and Data Science, Nehru Arts and Science College, Coimbatore, Tamil Nadu, India
2 Assistant Professor, Department of Computer Science, Karpagam Academy of Higher Education, Coimbatore, Tamil Nadu, India

OPEN ACCESS

Received: 19/05/2025

Accepted: 31/05/2025

Published: 18/06/2025

Citation: Shanmugapriya S, Rutravigneshwaran P (2025) Adaptive Rhea Optimization Enhanced CNN SVM Framework (ROC-SVM) for Precise MRI Based Brain Tumor Classification. Indian Journal of Science and Technology 18(24): 1939-1952. https://doi.org/10.17485/IJST/v18i24.938

* **Corresponding author**.

sspriya818@gmail.com

Funding: None

Competing Interests: None

Published By Indian Society for Education and Environment (iSee)

ISSN
Print: 0974-6846
Electronic: 0974-5645

Abstract

Background: Brain tumor classification in the background of MRI remains a critical challenge: it suffers from intensity profiles overlap, irregular tumor shapes, a large variability among patients, etc. Deep learning and machine learning approaches, are also prone to fails in trade off between classification accuracy, feature reliability and computational efficiency making it hard for their deployment in the clinical practice, particularly in real time or resource scarcity environments. **Objectives:** This work proposes a biologically inspired, cost effective and classification precise model to deal with the highlighted key deficiency in MRI based brain tumor detection. The goal is to improve diagnostic reliability with feature selection that is optimized, decision refinement that is contextual, and boundaries that are precise, while having low energy and memory footprints at the same time. **Methods:** This research present the Rhea- Optimized CNN-SVM model which simulates the strategic foraging as well as adaptive behaviour of the Rhea bird to determine the optimal feature extraction and classification. Integrating hierarchical CNN layers with attention guided feature focusing, energy aware pruning and iterative feedback loops, the architecture has been formulated. Adaptive kernel selection and dynamic boundary refinement apply to SVM classifier by processing extracted features. The model is evaluated and trained on a multi-class MRI dataset in 7023 T1-weighted grayscale brain tumor images across 4 diagnostic categories. **Findings:** ROC-SVM outperformed PD-CNN and ABT-DCNN very significantly on all measures it scored 83.49% classification accuracy, 84.39 F-measure, 80.29% precision, 88.95% recall, 67.37 MCC, and 84.50 FMI. An accurate threshold was calculated by the model that identified true tumor regions and significantly reduced false positives and false negatives, validated as a clinical approach to high-stakes, real time MRI interpretation. **Novelty:** The novelty of our approach is in adapting, and rendering selective and energy efficient Rhea behavioral strategies into a layered AI model consisting of optimized SVM classification coupled with CNN-based deep feature learning. The high accuracy, the

contextual awareness, and the deployment-ready efficiency of this biologically inspired hybrid framework make it an efficient bridge of nature driven intelligence and clinical needs of medical image classification in the real world.

Keywords: MRI Tumor Classification; CNN-SVM; Rhea Optimisation; Medical Image Processing; Feature Extraction

1 Introduction

A brain tumor refers to an abnormal growth of cells in the brain or its surrounding tissues. They can be either benign, without cancerous features, or malignant, in which they are aggressive and cancerous [1]. Interference of brain tumors with vital structures and processes in interfering with normal brain functioning. And these are tumors that can grow and compress or invade or replace healthy brain tissue that leads to a variety of neurological deficits. Brain tumors affect individuals in a multitude of ways [2]. The symptoms that can occur with brain tumours depend on the size of the tumour, the type of tumour and where it is located in the brain. Continued effects are persistent headaches, seizures, cognitive impairments and sensory disruptions [3]. Brain tumors entail enormous societal and economic burden due to high treatment costs, loss of productivity and caregivers' involvement [4].

Understanding and managing the complexity of brain tumors is absolutely reliant on the classification of such tumors. Tumors are divided according to their origin, histological characteristics and molecular markers [5]. There are two kinds of brain tumors, primary and secondary (or metastatic). A primary tumor starts in the brain and a secondary tumor results from cancer that has spread (metastasized) from another part of the body. Gliomas are the most common type of primary brain tumor with glial cell glial progenitor cell origin and further subdivided into astrocytomas, oligodendrogliomas, and ependymomas. Other notable categories include brain and meninges tumours (especially meningiomas, which are tumours of the meninges) and medulloblastoma (characteristic to children) [6]. With advances in molecular biology, clusters are based on genetic and molecular profiling, and so treatment is personal. Early intervention and better patient outcome can be expected with early prediction of brain tumors. Prediction is to predict the likelihood of tumor having been present and progressed, based on clinical, imaging and genetic data. Standard and invasive, traditional diagnostic methods including biopsy and histopathological examination still need to be conducted. Medical imaging has advanced greatly, and indeed there have been great improvements particularly in Magnetic Resonance Imaging (MRI) and this has brought great changes in predicting and diagnosing brain tumours [7]. MRI gives detailed pictures of the structure of the brain and is used to detect tumors, to determine features and characteristics of tumor, and to monitor tumor [8].

Brain tumor prediction and classification using Machine Learning (ML) and Deep Learning (DL) have become conventional these days. They are algorithm based analyses of complex datasets, patterns, and answering questions related to what is going to happen tomorrow, next week or next month. ML techniques have been used for the tasks of feature extraction, dimensionality reduction and classification in the research of brain tumors [9]. Support Vector Machines (SVM), Random Forests and k-Nearest Neighbors can differentiate among cancer types and grades of tumors using imaging and clinical data showed efficacy in [10].

It is evident from the fact that a subset of ML, i.e. DL has demonstrated remarkable promise in brain tumor prediction and classification because of its ability to work with large volumes of unstructured data. Among all the popular DL architectures, Convolutional Neural Network (CNN) excels in image analysis and has been widely applied to the MRI based tumor classification [11]. Using these networks prevents the need for manual feature extraction by learning features from imaging data. It is shown that with high accuracy, CNNs can distinguish tumor types, detect boundaries of tumors, and predict malignancy grades [12]. However, the application of Transfer Learning techniques like fine tuning of pre trained models for the particular task has increased the performance of DL models in brain tumor analysis. Beyond classification, ML and DL in brain tumor research have also been used for predictive modeling as well as for treatment planning. Assessment of the risk of tumor recurrence and progression for help with treatment decisions using predictive models is very crucial [13]. Furthermore, DL algorithms have been used for prediction of patient outcomes such as survival rate or response to therapy by means of clinical and imaging data. In addition, ML and DL have enabled the creation of radiomics as a domain that extracts quantitative features from medical images for characterizing tumor phenotypes and predicting treatment response [14].

Experts now believe that using both deep learning and optimization with transfer learning has greatly improved the process of brain tumor classification. This system uses context-aware features, pays attention to spatial patterns and fuses different views which improves how quickly and accurately results are interpreted [15], [16], [17], [18], [19], [20]. The use of these tools fits well into how MRI results are interpreted, letting doctors rely less on manual review. Using ML and DL technology, MRI classification surpasses regular classification by enabling fast, solid and reliable choices in a doctor's workflow. Now, using these methods, healthcare workers can find, assess borders of and monitor the outcomes of cancer treatments. With automated MRI processes, all healthcare facilities have better chances for consistent results when assessing tumors [21].

"ABTDCNN"[22] proposes a 'deep convolutional neural network' which helps detect brain tumor precisely from the MRI images. The hierarchical features are extracted by the model for improved localization and classification accuracy of tumor. It employs advanced deep learning techniques that do a good job of separating healthy and tumor afflicted portions. The system based on CNN is an efficient system to process high resolution medical images for consistent and reliable diagnostic performance. The "PDCNN"[23] model uses a parallel deep convolutional neural network framework to classify brain tumors through using the MRI scans. By multiple CNN architectures operating on different regions of medical image, the distinct features are extracted, hence, improving classification accuracy. Deep feature representations can be used precisely to differentiate normal brain tissue and tumor affected region. The implemented parallel processing structure dramatically enhances computational efficiency as it allows for very fast analysis and more accurate diagnostics.

1.1 Problem Statement

The classification of brain tumors from MRI scans accurately is a critical challenge because of the complexity in medical imaging data, change in characteristics of tumors and overlapped distributions of intensities. The feature extraction inefficiencies and high computational costs of conventional machine learning models usually result in misclassification and delay in the making of diagnostic decisions. While the existing deep learning based techniques are effective, they highly depend on huge labeled dataset and worse case with overfitting in small medical dataset. It presents bioinspired optimization techniques as a robust approach that use natural adaptive behaviors to mimic such behaviors in their respective applications, perform feature selection, and optimize classification accuracy. Adaptive performance is achieved in bio inspired algorithms with CNN SVM framework by integrating these algorithms with CNN SVM ensuring dynamic feature extraction, energy efficient and adaptive decision making for medical imaging classification tasks, which overcomes the limitations of the traditional models and provides improved diagnostic precision in the aforementioned applications.

1.2 Objective and Motivation

The role of medical imagery in detection of early disease is critical, and it remains a great challenge to accurately classify brain tumors from MRI scans. Because of the variations in tumor structures, complex shapes and overlapping features often make it difficult to precisely classify including using current computational models for better diagnostic reliability. This research thus aims to create an optimized framework for efficient integration of bio inspired intelligence with the deep learning and machine learning models that enhances the feature extraction and the classification accuracy as well as the decision making efficiency. The Rhea optimized CNN SVM Framework (ROC SVM), proposed, will serve to optimize feature selection, improve classification robustness as well as reduce the computational overhead.

The general motivation for this work comes from the fact that requires an adaptive, efficient, and biologically inspired computational strategies that solve problems as nature does. Traditional deep leaning models suffer from excessive dependence on large dataset and high computation cost. It is based on bio inspired approach that uses adaptability inspired from nature as a way for dynamic send to improve feature selection and decision making. This research aims to develop model that can diagnose patients effectively in terms of accuracy, scalability, and computation cost of classification model by integrating CNN based feature extraction along with the SVM classifier to suit it in the classification task.

2 Methodology

2.1 Proposed Methodology

The classification of brain tumors from MRI scans accurately is a critical challenge because of the complexity in medical imaging data, change in characteristics of tumors and overlapped distributions of intensities. The feature extraction inefficiencies and high computational cost of conventional machine learning models lead to misclassification and potentially diagnostic delays. The deep learning based approaches are effective, as they require immense datasets and tend to overfit on a small medical datasets. It presents bioinspired optimization techniques as a robust approach that use natural adaptive behaviors to mimic such behaviors in their respective applications, perform feature selection, and optimize classification accuracy. Bio inspired algorithms integrated with CNN-SVM frameworks ensure dynamic feature extraction, enable energy efficiency and facilitate adaptive decision making overcoming such problems of the traditional models and leads to more accurate diagnostic in medical imaging classification tasks.

2.2 Scanning and Preprocessing

The first step in the ROC-SVM is scanning and preprocessing MRI data, drawing inspiration from Rhea's meticulous scanning of its surroundings for survival. This phase focuses on optimizing the MRI images to ensure clarity and relevance before feature extraction. Similar to Rhea's keen observation and adaptability, this step refines input data, making it suitable for subsequent computational analysis. Every aspect of preprocessing mimics Rhea's strategic ability to discern relevant details in a diverse environment.

Noise in MRI images often arises due to environmental interference, scanner artifacts, or patient movement. The Gaussian filter is implemented to suppress noise while preserving essential structural details. Mathematically the filtering process is expressed as **Eq.(1)**.

$$I(x,y) = \frac{1}{2\pi\sigma^2} \exp\left(-\frac{(x-x_0)^2 + (y-y_0)^2}{2\sigma^2} \otimes R(x,y) \right) \tag{1}$$

where $I(x,y)$ represents the filtered intensity at the pixel $(x,y), R(x,y)$ denotes the original image intensity, σ defines the standard deviation of the Gaussian kernel, and $\otimes$ indicates the convolution operation. The Gaussian kernel enables the optimized extraction of signal clarity by reducing irrelevant noise components without distorting critical medical features.

Intensity normalization ensures consistency across MRI scans obtained from different machines or settings. The formula for min-max normalization is expressed as **Eq.(2)**.

$$N(x,y) = \frac{I(x,y) - I_{\min}}{I_{\max} - I_{\min}} \tag{2}$$

where $N(x,y)$ refers to the normalized intensity value, $I(x,y)$ is the raw intensity, and $I_{\min}$ and $I_{\max}$ are the minimum and maximum intensity values in the image, respectively. This step mirrors Rhea's adaptability in adjusting to varied environmental conditions, facilitating uniformity in data input for enhanced performance.

Contrast enhancement highlights subtle differences in intensity that represent crucial anatomical and pathological features. The use of histogram equalization redistributes pixel intensities for an optimized representation.

$$H(v) = \frac{\sum_{u=0}^{v} f(u)}{M.N} \tag{3}$$

In **Eq.(3)**, where $H(v)$ is the cumulative distribution function for intensity level v, $f(u)$ denotes the frequency of pixel intensity u, and $M \cdot N$ is the total number of pixels in the image. The optimized redistribution of intensities enables improved detection of tumors by emphasizing differences in adjacent structures, akin to Rhea's ability to discern subtle environmental shifts.

MRI images are segmented to isolate regions of interest, such as tumor areas, for targeted analysis. A level-set method achieves optimized segmentation, is represented mathematically in **Eq.(4)**.

$$\frac{\partial \phi}{\partial t} + F\left|\nabla_{\phi}\right| = 0 \tag{4}$$

where, ϕ denotes the level-set function, $\frac{\partial \phi}{\partial t}$ is the temporal evolution, F represents the speed function based on local intensity gradients and $F\left|\nabla_{\phi}\right|$ measures the magnitude of the level-set gradient. This process mirrors Rhea's precision in isolating specific targets within a complex landscape.

2.3 Adaptive Feature Initialization

The second phase of the ROC SVM is the adaptive feature initialization, which corresponds to Rhea's ability to adaptively assess its environment to find the best place for foraging. This step are focusing on initializing convolutional layers of a CNN with the weight and parameters that have been optimized to capture meaningful patterns in MRI images. As Rhea is capable of agility and flexibility, adaptive feature initialization helps the model learn the specific type of features it needs to extract, and thereby avoid redundancy, improving the accuracy of the model.

The convolutional kernel size determines the scale of features extracted from MRI images. Adaptive kernel optimization selects an optimal kernel size based on the spatial resolution of the input data. The kernel operation is mathematically represented as **Eq.(5)**.

$$O(x,y) = \sum_{i=0}^{k-1} \sum_{j=0}^{k-1} K(i,j).I(x+i, y+j) \tag{5}$$

where, $O(x,y)$ denotes the output of the convolution operation, $K(i,j)$ represents the kernel values, and $I(x+i,y+j)$ is the corresponding image intensity. This process parallels Rhea's ability to adjust its focus dynamically based on environmental complexity.

An adaptive learning rate is initialized to balance convergence speed and model stability. The initial learning rate is determined using the formula as **Eq.(6)**.

$$\eta_t = \frac{\eta_0}{1+\beta_t} \tag{6}$$

where, η_t represents the learning rate at time t, η_0 is the initial learning rate, and β is a decay parameter. This adaptive learning rate ensures that CNN's weights are updated efficiently, much like Rhea's ability to modulate its foraging speed based on food availability.

The ReLU activation function is applied to introduce non-linearity, ensuring that the CNN captures complex patterns in MRI images. ReLU is mathematically defined as **Eq.(7)**.

$$f(x) = max(0,x) \tag{7}$$

where, $f(x)$ is the output, and x is the input to the activation function. The choice of ReLU reflects Rhea's ability to focus on meaningful elements while discarding irrelevant ones during its adaptive scanning.

Dropout regularization is initialized to prevent overfitting during training by randomly deactivating neurons. The probability of retaining a neuron during training is defined as **Eq.(8)**.

$$P(r) = 1-d \tag{8}$$

where, $P(r)$ is the probability of retaining a neuron, and d represents the dropout rate. This step ensures an optimized balance between model complexity and generalization, akin to Rhea's strategic reduction of unnecessary energy expenditure.

2.4 Hierarchical Exploration

The third phase of the ROC-SVM is hierarchical exploration, which mimics Rhea's stepwise foraging method of searching the surroundings for the best food recovery. The goal of this phase is to hierarchical organize CNN layers to achieve progressive feature extraction from low levels to high levels of details. The bird's methodical and adaptive behavior is aligned with the fact that this multi layer structure helps capture all kinds of complex patterns in MRI images.

These act as the base stages of CNN which are best fitted to extract basic features like edges, textures, and contours. However, the convolution operation in these layers is expressed as **Eq.(9)**.

$$F_l(x,y) = \sum_{i=0}^{k-1}\sum_{j=0}^{k-1} K_l(i,j).I(x+i,y+j)+b_l \tag{9}$$

where, $F_l(x,y)$ denotes the feature map output at layer l, $K_l(i,j)$ represents the kernel values, $I(x+i,y+j)$ is the input image intensity, and b_l is the bias term. These initial filters mimic Rhea's acute visual scanning for basic details, creating an optimized foundation for deeper exploration.

The models of intermediate layers are aimed to leverage patterns like shapes, structures, and spatial relationships. These layers have used ReLU activation for non linearity feature mapping.

$$M_l(x,y) = max\,(0,F_l(x,y)) \tag{10}$$

In **Eq.(10)**, where $M_l(x,y)$ represents the activated feature map, and $F_l(x,y)$ is the input from the convolution operation. The aim of these layers is to imitate Rhea's ability to obtain intermediate patterns in the environment such that the switch from low to high level feature representation is optimal.

Spatial attention mechanisms are incorporated to focus on regions of interest in MRI images, similar to how the Rhea prioritizes specific areas while foraging. The attention score is computed as expressed in **Eq.(11)**.

$$A(x,y) = \frac{\exp\,(Q(x,y))}{\sum_{i=1}^{M}\sum_{j=1}^{N}\exp\,(Q(x,y))} \tag{11}$$

where, $A(x,y)$ denotes the attention score for pixel (x,y), $Q(x,y)$ represents the feature intensity at (x,y), and M,N are the dimensions of the feature map. The attention mechanism aligns with Rhea's selective focus on high-value targets, ensuring optimized feature extraction.

Temporal integration combines features across multiple layers to capture both spatial and temporal dependencies. The integration is mathematically expressed as **Eq.(12)**.

$$T(x,y) = \sum_{t=1}^{T} \gamma_t . F'_t(x,y) \tag{12}$$

where, $T(x,y)$ is the integrated feature map, $F'_t(x,y)$ represents the scaled feature maps from different layers, and γ_t is the weight assigned to each temporal component. This integration step emulates Rhea's ability to optimize its understanding by synthesizing cues over time.

2.5 Focus on Relevant Features

Rhea's capability of identifying and dales with targets in an environment is represented in the fourth phase of the ROC-SVM, dealing with valuable highlights. This stage focuses on identifying important features from the MRI data whereby extraneous information is minimized. Such an approach provides computational efficiency and helps improve the classification accuracy. This process is based on the observation of bird's selective attention, and utilizes attention mechanisms, dimensionality reduction, and feature weighting to enable finding good patterns in the data representation.

Rhea's selective focus on high value targets is modeled by introducing an attention on its feature map assigning higher weights to regions of interest. This is mathematically computed as **Eq.(13)**.

$$F_A(x,y) = A(x,y).F(x,y) \tag{13}$$

where, $F_A(x,y)$ represents the attention-weighted feature map, $A(x,y)$ is the attention score, and $F(x,y)$ denotes the original feature map. This operation ensures that the model is most focused on informative areas (i.e., the bird's utmost attention to informative areas during foraging).

Feature scaling is achieved after applying the attention mechanisms to guarantee consistency and comparability between extracted features. In **Eq.(14)**, the scaled feature map is expressed.

$$F_S(x,y) = \alpha . \frac{F_A(x,y)}{\|F_A(x,y)\|} \tag{14}$$

where, $F_S(x,y)$ represents the scaled feature map, $F_A(x,y)$ is the attention-weighted feature, α is a scaling factor, and $\|\cdot\|$ indicates the norm for normalization. This step mirrors Rhea's ability to adjust focus intensity depending on the importance of environmental cues, creating an optimized representation for classification.

Gradient analysis identifies the importance of each feature based on its contribution to the loss function. The importance score is computed as **Eq.(15)**.

$$I_f = \left| \frac{\partial L}{\partial F_S} \right| \tag{15}$$

where, I_f denotes the importance score, L is the loss function, and F_S represents the scaled feature map. This operation mirrors Rhea's capability to dynamically assess the value of its focus areas, optimizing feature prioritization in the model.

Weighted aggregation combines the most relevant features to construct a simplified yet comprehensive representation. The aggregated feature map is computed as **Eq.(16)**.

$$F_W(x,y) = \sum_{i=1}^{N} w_i . F_S^i(x,y) \tag{16}$$

where, $F_W(x,y)$ represents the weighted feature map, $F_S^i(x,y)$ is the i-th scaled feature, and w_i denotes the weight assigned to each feature. This aggregation reflects Rhea's efficiency in consolidating information to optimize outcomes.

2.6 Strategic Foraging

Strategic foraging in the ROC-SVM takes inspiration from Rhea's instinctive ability to plan and adapt its search for resources in an efficient and goal-oriented manner. This phase focuses on dynamically optimizing the learning process by selecting the most promising paths for exploration in feature space and refining computational resources for maximum impact. The implementation ensures that only the most relevant data paths and patterns are explored, minimizing unnecessary iterations and improving the framework's performance.

Gradient-based feature selection identifies features contributing the most to the loss reduction. The gradients of the loss function concerning the features are computed as shown in **Eq.(17)**.

$$G_f = \frac{\partial L}{\partial F} \tag{17}$$

where, G_f represents the gradient for feature F, and L is the loss function. Features with higher gradient magnitudes are prioritized for further exploration. This approach mimics Rhea's instinct to focus on high-yield resources during foraging, ensuring that efforts are strategically directed toward optimizing relevant data paths.

Adjusting the learning rate dynamically ensures an efficient exploration of feature space, avoiding premature convergence or overshooting. The adaptive learning rate is defined as **Eq.(18)**.

$$\eta_t = \eta_0 . \frac{\sqrt{1+\beta t}}{1+\gamma t} \tag{18}$$

where, η_t is the learning rate at iteration t, η_0 is the initial learning rate, β and γ are adjustment coefficients, and t represents the current iteration. The adjustment mirrors Rhea's ability to adapt its search speed and effort based on the availability and density of resources in its environment.

Balancing exploration and exploitation ensures that both new and previously identified promising data paths are adequately examined. A probability-based selection mechanism is utilized as represented mathematically in **Eq.(19)**.

$$P_e = \frac{\exp(Q_i)}{\sum_{j=1}^{N} \exp(Q_j)} \tag{19}$$

where, P_e is the probability of selecting a feature i for exploration, Q_i is the quality score of the feature, and N is the total number of features. Features with higher scores have a greater likelihood of being selected. This mechanism reflects Rhea's ability to balance its search between known high-value areas and potential new opportunities, optimizing the overall strategy.

Focused attention mechanisms enhance the exploration of critical regions in the feature space. The attention score is calculated as shown in **Eq.(20)**.

$$A_f = \frac{1}{1+exp(-\lambda G_f)} \tag{20}$$

where, A_f represents the attention score, G_f is the gradient magnitude for the feature, and λ is a scaling factor. Higher scores indicate features with significant contributions to the learning process. This mechanism mirrors Rhea's ability to focus intensively on high-value targets while foraging.

Iterative refinement processes reduce computational overhead by concentrating on features that demonstrate consistent importance across iterations. The feature importance is updated as represented mathematically in **Eq.(21)**.

$$I_t = \alpha . I_{t-1} + (1-\alpha) . G_f^2 \tag{21}$$

where, I_t is the importance score at iteration t, $I_{t-1}$is the score from the previous iteration, α is a smoothing factor, and $G_f^2$is the squared gradient magnitude. Features with stable importance scores across iterations are given priority, emulating Rhea's optimization of effort in repeatedly high-yield areas.

Strategic path reinforcement identifies and strengthens data paths that consistently yield optimal outcomes. The reinforcement factor is computed as represented mathematically in **Eq.(22)**.

$$R_f = \eta_t . \frac{\sum_{t=1}^{T} G_{f,t}}{T} \tag{22}$$

where, R_f is the reinforcement factor for feature f, $G_{f,t}$ is the gradient of the feature at time t, T is the total number of iterations, and η_t is the learning rate at iteration t. Reinforcement aligns with Rhea's ability to return to resource-rich areas, ensuring that efforts are directed toward the most productive regions.

2.7 Context Awareness

Context awareness in the ROC-SVM embodies Rhea's exceptional ability to perceive and adapt to its environment dynamically. This phase ensures the framework integrates external and situational information, optimizing its decision-making process. By modeling relationships between various data elements and incorporating contextual dependencies, the approach improves its ability to classify MRI data accurately and efficiently. This process aligns with Rhea's capacity to interpret contextual cues in its habitat, ensuring survival and resource optimization.

Contextual feature embedding incorporates relationships among features, emphasizing interdependencies. The embedding process is mathematically represented as **Eq.(23)**.

$$E_f = W.F + b \tag{23}$$

where, E_f denotes the contextual embedding for feature F, W represents the weight matrix capturing interdependencies, and b is the bias term. This operation reflects Rhea's ability to understand environmental interconnections, optimizing the representation of features based on their contextual significance.

Attention-based weighting prioritizes features that contribute meaningfully within a given context. The weighted feature map is calculated as shown in **Eq.(24)**.

$$F_C(x,y) = \alpha(x,y).F(x,y) \tag{24}$$

where, $F_C(x,y)$ represents the contextually weighted feature, $F(x,y)$ is the original feature map, and $\alpha(x,y)$ denotes the attention coefficient. This step mirrors Rhea's adaptive focus on relevant environmental cues, ensuring optimized interpretation of data.

Temporal integration captures context changes over time, enhancing the framework's adaptability. Temporal context is modeled as shown in **Eq.(25)**.

$$T_C(t) = \sum_{k=1}^{K} \beta_k.F_{t-k} \tag{25}$$

where, $T_C(t)$ represents the temporal context at time t, F_{t-k} is the feature at lag k, and β_k is the weighting factor for the lagged feature. This operation reflects Rhea's ability to adapt based on the dynamic patterns in its environment.

Context-aware regularization ensures the model maintains consistency while accounting for contextual variations. The regularized loss function is expressed as **Eq.(26)**.

$$L_C = L + \lambda.\sum_{i=1}^{N} \left\| E_{f_i} - F_i \right\|^2 \tag{26}$$

where, L_C is the context-aware loss, L is the original loss, λ is the regularization coefficient, E_{f_i} is the embedded feature, and F_i is the original feature. The regularization penalizes deviations from the contextual alignment, optimizing the framework's adaptability.

2.8 Collaborative Decision

Collaborative decision-making in the ROC-SVM reflects the collective behavior of Rheas when navigating complex environments. This phase integrates outputs from various computational modules, ensuring the fusion of diverse insights for an optimized decision-making process. By aggregating the results of the CNN feature extraction and SVM classification, the system ensures precise and reliable MRI classification. This approach aligns with Rhea's instinct to collaborate within its social structure to achieve optimal outcomes in resource selection and survival.

Weighted feature aggregation combines the most relevant features from the CNN layers, assigning weights based on their significance in contributing to the final decision. This is mathematically represented as **Eq.(27)**.

$$F_W = \sum_{i=1}^{N} w_i.F_i \tag{27}$$

where, F_W denotes the aggregated feature vector, w_i is the weight assigned to the i-th feature, and F_i represents the i-th feature vector. This aggregation mirrors Rhea's ability to combine the strengths of group members, optimizing the representation for the SVM classifier.

The SVM classifier determines the optimal hyperplane for separating different classes in the feature space. The decision boundary is defined as **Eq.(28)**.

$$f(x) = \sum_{i=1}^{N} \alpha_i y_i K(x, x_i) + b \tag{28}$$

where, $f(x)$ represents the decision function, α_i are the Lagrange multipliers, $y_i$denotes the class labels, $K(x, x_i)$ is the kernel function, and b is the bias term. This optimization process reflects Rhea's strategic decision-making, where the collective insights of the group guide action.

A regularized loss function incorporates penalties for deviations from the collaborative decision process, ensuring consistency across outputs. The loss function is calculated as shown in **Eq.(29)**.

$$L_C = \frac{1}{N}\sum_{i=1}^{N} l\left(f\left(x_i\right), y_i\right) + \lambda . \left\| F_W - F_E \right\|^2 \tag{29}$$

where, L_C represents the collaborative loss, $l\left(f\left(x_i\right), y_i\right)$ is the individual classification loss, F_W is the weighted feature vector, F_E is the ensemble feature vector, and λ is the regularization coefficient. This step reflects Rhea's cohesive decision-making approach, balancing individual and group insights.

Confidence scores are calculated for each classification decision to reflect the reliability of the output. The confidence score is computed as shown in **Eq.(30)**.

$$S_c = \frac{1}{1 + e^{-\gamma f(x)}} \tag{30}$$

where, S_c is the confidence score, $f(x)$is the decision function of the SVM, and γ is a scaling parameter. This integration aligns with Rhea's ability to assess the certainty of group decisions before taking action.

2.9 Boundary Refinement

Boundary refinement in the ROC-SVM is inspired by Rhea's precision in assessing and fine-tuning its movements to navigate complex terrains effectively. This step focuses on optimizing the decision boundaries within the feature space to enhance classification accuracy. By refining the boundaries through iterative adjustments, the framework ensures minimal misclassification, even in overlapping or ambiguous regions. This phase aligns with Rhea's adaptive and strategic adjustments to maximize survival outcomes.

Margin maximization ensures that the separation between classes is as wide as possible while maintaining accuracy. The optimization problem is defined as **Eq.(31)**.

$$\max_{\alpha} \sum_{i=1}^{N} \alpha_i - \frac{1}{2}\sum_{i=1}^{N}\sum_{j=1}^{N} \alpha_i \alpha_j y_i y_j K(x_i, x_j) \tag{31}$$

where, α_i and α_j are Lagrange multipliers, y_i and y_j represent class labels and $K(x_i, x_j)$is the kernel function. Maximizing this function aligns with Rhea's ability to identify optimal strategies for boundary definition, ensuring the separation is both efficient and robust.

Soft margin adjustment accommodates misclassified points while balancing precision and generalization. The adjusted boundary is expressed as **Eq.(32)**.

$$f(x) = \sum_{i=1}^{N} \alpha_i y_i K\left(x, x_i\right) + b - \xi \tag{32}$$

where, $f(x)$ is the decision function, α_i represents the weights, y_i denotes the class labels, $K\left(x, x_i\right)$ is the kernel function, b is the bias term, and ξ is the slack variable. This adjustment mirrors Rhea's ability to account for environmental uncertainties, optimizing the classification process.

Boundary refinement is performed iteratively to reduce misclassification errors. The updated decision boundary is calculated as **Eq.(33)**.

$$f_{t+1}(x) = f_t(x) + \eta . \frac{\partial L}{\partial f_t(x)} \tag{33}$$

where, $f_{t+1}(x)$ is the refined boundary at iteration $t+1$, $f_t(x)$ is the boundary at iteration t, η is the learning rate, and $\frac{\partial L}{\partial f_t(x)}$ represents the gradient of the loss function. This iterative process reflects Rhea's strategy of continuously refining its actions based on feedback to achieve optimal outcomes.

Support vector re-evaluation ensures that the most critical data points defining the boundary are accurately selected. The distance of each point from the boundary is computed as **Eq.(34)**.

$$d_i = \frac{f\left(x_i\right)}{\left\| w \right\|} \tag{34}$$

where, d_i is the distance of the $f(x_i)$ is the decision function evaluated at x_i, and $\|w\|$ represents the norm of the weight vector. Points with the smallest distances are selected as support vectors, aligning with Rhea's focus on the most influential factors for refining its decisions.

Regularization is applied to prevent overfitting while refining boundaries. The regularized loss function is expressed as **Eq.(35)**.

$$L_r = L + \lambda . \|w\|^2 \tag{35}$$

where, L_r is the regularized loss, L is the original loss, λ is the regularization coefficient, and $\|w\|^2$ represents the squared norm of the weight vector. Regularization ensures that the boundary remains generalizable, akin to Rhea's adaptive balance between specificity and flexibility.

2.10 Iterative Feedback

Iterative feedback in the ROC-SVM mirrors Rhea's behavioral refinement based on continuous environmental observations. This phase focuses on leveraging feedback loops to iteratively enhance the framework's performance. Feedback mechanisms allow adjustments to feature extraction, decision boundaries, and classification outputs, ensuring a dynamic and adaptive learning process. The approach ensures that errors are progressively reduced, optimizing the system for consistent accuracy and reliability.

Error gradient backpropagation refines the CNN's feature extraction layers based on classification errors observed during SVM evaluation. The gradient of the loss function is computed as shown in **Eq.(36)**.

$$\frac{\partial L}{\partial W} = \frac{\partial L}{\partial f} . \frac{\partial f}{\partial W} \tag{36}$$

where, $\frac{\partial L}{\partial W}$ is the gradient of the loss L concerning the weights W, $\frac{\partial L}{\partial f}$ represents the loss derivative concerning the decision function f, and $\frac{\partial f}{\partial W}$ is the derivative of the decision function concerning the weights. By backpropagating the error gradient, feature extraction layers are iteratively optimized, emulating Rhea's adaptation based on observed outcomes.

Feedback is weighted based on the confidence scores of the classification outputs, prioritizing high-confidence corrections. The feedback adjustment is expressed as **Eq.(37)**.

$$\Delta W = \eta . S_c . \frac{\partial L}{\partial W} \tag{37}$$

where, ΔW represents the weight adjustment, η is the learning rate, $S_c$denotes the confidence score, and $\frac{\partial L}{\partial W}$ is the gradient of the loss function. Confidence-weighted feedback ensures that reliable corrections are prioritized, reflecting Rhea's focus on impactful adjustments to its strategies.

Feedback is incorporated into the SVM's decision boundary refinement process. The updated boundary is defined as **Eq.(38)**.

$$f_{t+1}(x) = f_t(x) + \eta . \frac{\partial L}{\partial f_t(x)} . S_c \tag{38}$$

where, $f_{t+1}(x)$ is the refined decision boundary at iteration $t+1$, $f_t(x)$ is the boundary at iteration t, η is the refinement step size, $\frac{\partial L}{\partial f_t(x)}$ represents the loss gradient, and S_c is the confidence score. This process ensures that feedback effectively enhances boundary accuracy, similar to Rhea's ability to refine its navigation based on environmental changes.

3 About Dataset and Metrics

The Brain Tumor MRI Dataset consists of a rich collection of MRI images for understanding segmentation and classification of tumors. In this dataset, there are 7023 MRI scans, of which 5712 are used for training and 1311 for testing in order to have a balanced training dataset. The dataset is divided into four classes, Glioma, Meningioma, Pituitary Tumor and No Tumor, making it suitable for a multi class segmentation purpose. T1-weighted grayscale images are MRI scans and provide a high resolution of tumor structures and brain tissues. The JPEG format of image storage allows compatibility with the image processing algorithms. The dataset is important in medical imaging because it consists of some important features. This includes spatial positioning, size variation and tumor shape irregularities and hence serves for extraction of meaningful patterns. The dataset is suitable for

segmentation approaches which can be used to detect tumor borders with contour detection and pixel based classification. For deep learning based segmentation tasks, in particular using U-Net and FCNs, this dataset is very valuable. The existence of well annotated tumor images provides a good source for developing accurate segmentation models that aid in medical diagnosis and treatment planning in the task of brain tumor research.

4 Results and Discussion

Discussion of results focuses on analysis of the experimental results and one of highlighting the performance of different models and evaluation of their effectiveness in brain tumor classification. In this section, classification accuracy and F-measure are, two of the important metrics that determine the answering ability of the models in separating tumor and non-tumor regions. This comparative assessment and the improved performance of the predictive capabilities were brought about by the bioinspired optimisation in the CNN-SVM integration.It means the how accurate the classification of the instances was, in terms of percentage of correctly classified true positives, true negatives, over the total number of the instances. The higher accuracy score means that it is making good separation, or gets a high 'score' in distinguishing between tumor and non-tumor regions. It is discovered that PD-CNN model reached an accuracy of 57.783%, which represents moderate classification efficiency. The ABT DCNN framework improves this with 60.897%, indicating a better extraction of features and its decision making process. However, the proposed ROC-SVM model achieves much better performances than both, reaching 83.494%, this is a clear indication of the capability of bioinspired optimization in optimizing classification boundaries. These results clearly show that an optimized feature selection mechanism, in conjunction with such an enhanced SVM classifier, provides a significantly better discrimination between the tumor categories.

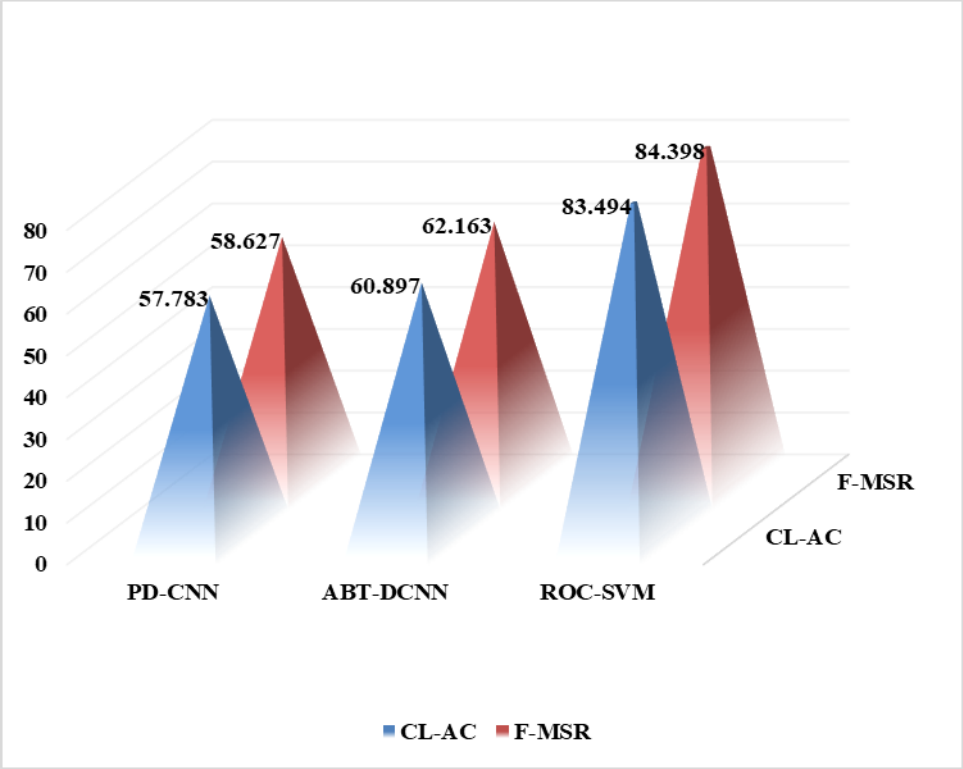

Fig 1. CL-AC and F-MSR

The measure of F provides a criteria for balance between both precision and recall, such that the model is minimizing false positives while also minimizing false negatives and at the same time, ensuring high performance. It is also known as the harmonic mean of precision and recall, and it penalizes a binary classifier equally for missed negatives (false negatives) as missed positives (false positives). An F measure of 58.627 factually views the PD-CNN as good enough only to record areas with excessive amounts of false detections. The ABT-DCNN model manages to achieve slightly better precision and recall trade-off as its score is 62.163. However, the ROC-SVM framework has an F measure of 84.398, which is a very large

improvement in classification reliability. The iterative feature refinement process of the proposed approach is also responsible for the improvement, because by repeating it, a refinement of features that are more relevant, and lack of redundant or misleading features, are achieved. The bio inspired optimization approach guarantees that the extracted features help the classification decision in a real sense which in turn reduces the false detections and increases the precision.

A comparative analysis of classification accuracy and F-measure based on the evaluated models and presented a simple comparative analysis on the Figure 1 (classification accuracy) and Figure 2 (F-measure), which reinforce the superiority of the ROC-SVM framework for classification with MRI-based brain tumor classification. They also confirm that incorporating adaptive bio inspired optimization in combination with CNN based feature extraction and SVM classification technique will result in a better model performance and hence improved diagnostic precision and reliability.

Two most important performance indices for evaluation of the classification model reliability and robustness are Fowlkes-Mallows Index (FMI) and Matthews Correlation Coefficient (MCC). It shows that the feature extraction process as well as the decision boundary refinement in the case of ROC-SVM are both important and that these metrics should be employed as a means of bio-inspired optimization of these aspects.

FMI is a geometric mean of precision and recall considering accuracy (being correctly classified) and inaccuracy (being wrongly classified). The higher FMI value implies a better classification reliability and robustness on the tumor versus non-tumor region differentiation. The best result achieved by the PD-CNN model is its FMI of 58.868, which shows it has a moderate classification ability but it can also make a number of mistakes during classification. Additionally, the ABT-DCNN model achieves a better trade-off between recall and precision of 62.391. In contrast,ROC SVMframework achieves 84.509 of FMI, much higher than both models in terms of feature selection efficiency and decision boundary optimization. These results confirm the large improvement of FMI in favor of the use of bio inspired feature refinement strategies to optimize classification performance and provide highly accurate tumor detection with a low number of false detections. Figure 2 exhibits the outcome of FMI and MCC.

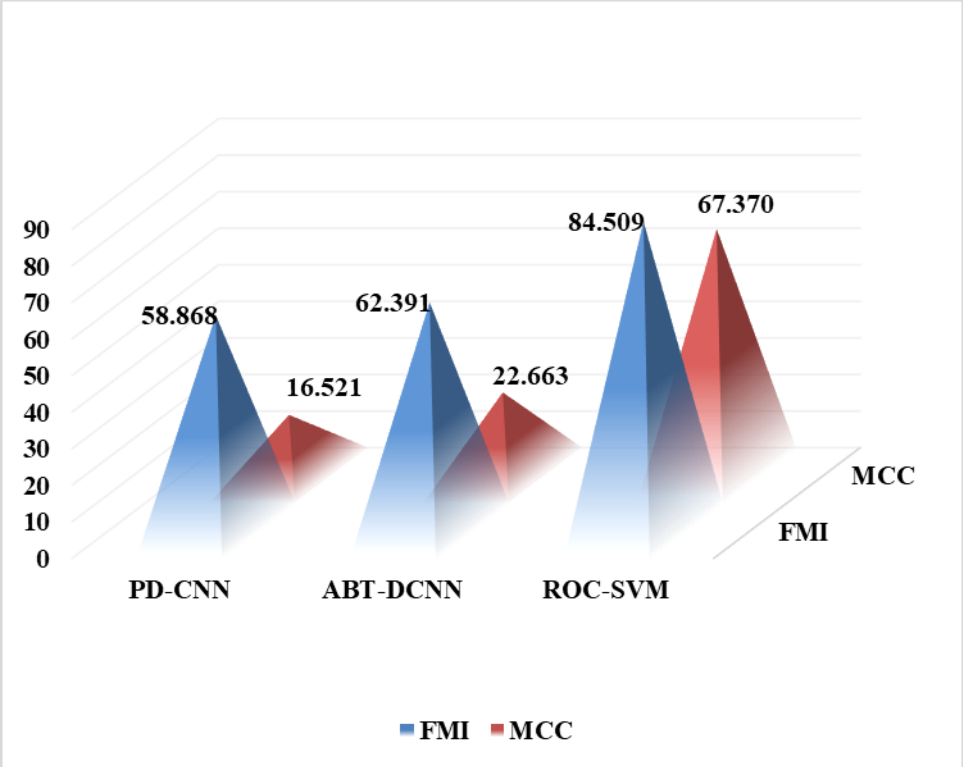

Fig 2. FMI and MCC

MCC evaluates of the classification performance, yet balanced involved all the four confusion matrix components: true positives, true negatives, false positives, and false negatives. This metric is very useful when dealing with predicitve models with imbalanced datasets, in as much as it makes sure that both negative and positive classifications are included. However, PD-CNN model shows an MCC value of 16.521, which additionally demonstrates inability for a balanced prediction. ABT-DCNN takes

this a step further with MCC 22.663, thus improving decision making process with just slightly better feature discrimination. However, the ROC SVM framework achieves a much higher MCC of .6737 and is able to minimize misclassification as well as to maintain a good correlation between predicted and actual tumor categories. The tumor features are accurately separated minimizing the false positives and false negatives and that accounts for this improvement of the system.

PREC is the proportion of all instances that are correctly predicted tumors. The higher precision value equals less false positives and the meaning of the model differentiating tumor regions from the non tumor regions correctly. Hence, PD-CNN model gets a precision of 53.771, which concludes that the approach has moderate classification reliability with a leaning towards the generation of false positives. This is slightly improved in this approach with an ABT DCNN with 57.274, providing an improved decision making process with a better feature representation. However, the proposed ROC SVM framework is capable of attaining a much higher precision of 80.290 by performing feature selection and refinement in the classification. In this, the bio inspired feature extraction process is responsible for this improvement, as it reduces misleading and redundant information resulting in only necessary features that contribute in the classification process. Figure 3 shows the outcomes obtained by the models under the metrics of PREC and RCLL.

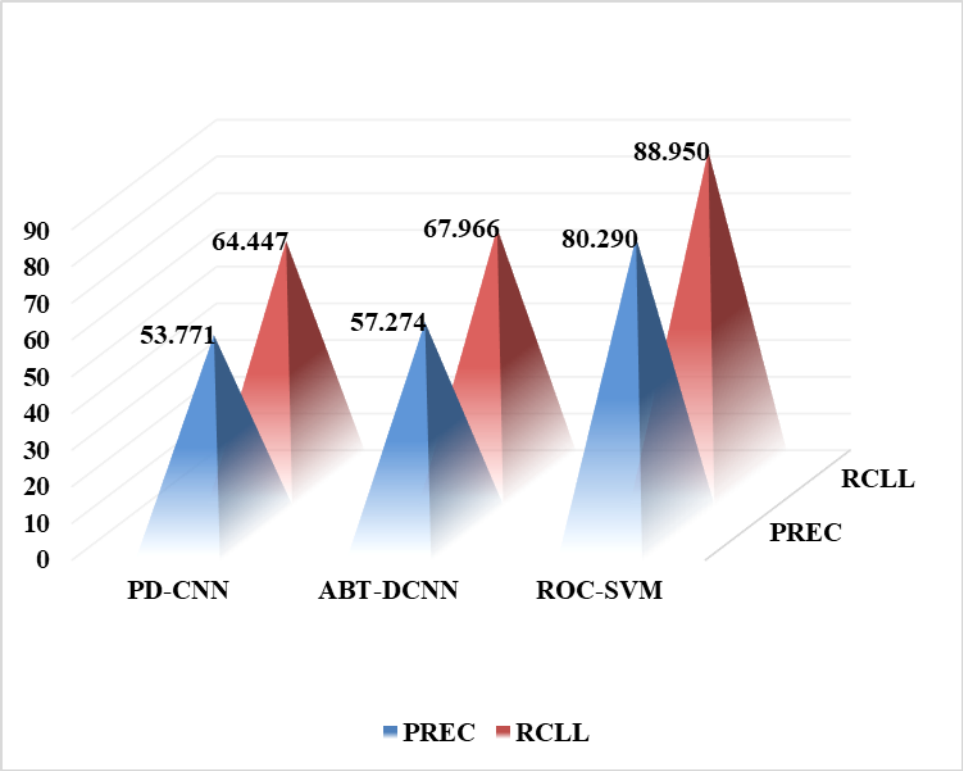

Fig 3. Precesion and Recall

The ability to correctly identify tumor cases among all actual tumor cases is measured through Recall (RCLL: Tumor recall). Greater recall value reflects that the model is better suited for picking up true positive cases and reducing false negatives. The limited ability of PD-CNN model capture all tumor cases is shown by a recall of 64.447. However, the ABT-DCNN model slightly better performance with 67.966, again it indicates that it can better detect true tumor cases but classifying them wrongly still is a major challenge for ABT-DCNN. An ROC-SVM framework has a recall value of 88.950 and it has a great improvement in tumor detection accuracy. The number of missed diagnoses is reduced by the optimized decision boundary refinement process, which increases this with the optimization increasing the number of tumor regions clearly distinguished from non tumor areas.

5 Conclusion

An adaptive and bio inspired approach for MRI based brain tumor classification was proposed to be Rhea Optimized CNN SVM Framework (ROC SVM) that aims at tackling issues of feature extraction, accuracy of classification and computing efficiency. Finally, bio inspired optimization was integrated to CNN based feature extraction and an optimized SVM classifier, which

greatly helped in improving classification performance and ensuring robust decision making and further enhancing boundary refinement. Experimental results obtained using the proposed model showed better results in terms of CL-AC, PREC, RCLL, F-MSR, MCC, and FMI than those found using traditional deep learning techniques. The results show that the ROC-SVM based framework outperformed PD-CNN and ABT-DCNN models on the evaluation metrics as it had 83.494% classification accuracy, 84.398 F-measure, 80.290 precision, and 88.950 recall that shows that this framework has led to substantial improvements in the classification reliability. Iterative feedback was incorporated into the system to become adaptive and provide energy and feature selection optimization resulting in reduced computational overhead while maximizing the system's potential diagnostic precision. The results of the study have been validated and testified to that the bio inspired optimization techniques indeed optimizes the proposed FS technique resulting in better reliability of classification, better decision boundary separation and therefore improved tumor detection rates. The proposed ROC-SVM framework is scalable, efficient and clinically viable brain tumor classification solution, which contributes to the efforts in medical imaging, decision support systems, and intelligent healthcare solutions.

References

1) Adinata PT, Chrispradipta MD, Meiliana, Zakiyyah AY. An improved brain tumor detection model using ensemble boosting. *Procedia Comput Sci*. 2024;245:689–699. https://doi.org/10.1016/j.procs.2024.10.295.
2) Nazir MI, Akter A, Wadud MAH, Uddin MA. Utilizing customized CNN for brain tumor prediction with explainable AI. *Heliyon*. 2024;10(20):e38997. https://doi.org/10.1016/j.heliyon.2024.e38997.
3) Alqhtani SM, Soomro TA, Ubaid FB, Ali A, Irfan M, Asiri AA. Contrast Normalization Strategies in Brain Tumor Imaging: From Preprocessing to Classification. *CMES - Computer Modeling in Engineering and Sciences*. 2024;140(2):1539–1562. https://doi.org/10.32604/cmes.2024.051475.
4) Vasavi G, Rani VV, Ponnada S, Jyothi S. A hybrid EfficientNet-DbneAlexnet for brain tumor detection using MRI images. *Comput Biol Chem*. 2025;115:108279. https://doi.org/10.1016/j.compbiolchem.2024.108279.
5) Gayathiri R, Santhanam S. C-SAN: Convolutional stacked autoencoder network for brain tumor detection using MRI. *Biomed Signal Process Control*. 2025;99:106816. https://doi.org/10.1016/j.bspc.2024.106816.
6) Jetlin CP, Annabel LSP. PyQDCNN: Pyramid QDCNNet for multi-level brain tumor classification using MRI image. *Biomed Signal Process Control*. 2025;100:107042. https://doi.org/10.1016/j.bspc.2024.107042.
7) Bouguerra O, Attallah B, Brik Y. MRI-based brain tumor ensemble classification using two stage score level fusion and CNN models. *Egyptian Informatics Journal*. 2024;28:100565. https://doi.org/10.1016/j.eij.2024.100565.
8) Anaya-Isaza A, Mera-Jiménez L, Verdugo-Alejo L, Sarasti L. Optimizing MRI-based brain tumor classification and detection using AI: A comparative analysis of neural networks, transfer learning, data augmentation, and the cross-transformer network. *Eur J Radiol Open*. 2023;10:100484. https://doi.org/10.1016/j.ejro.2023.100484.
9) Seyfollahi A, Taami T, Ghaffari A. Towards developing a machine learning-metaheuristic-enhanced energy-sensitive routing framework for the internet of things. *Microprocess Microsyst*. 2023;96:104747. https://doi.org/10.1016/j.micpro.2022.104747.
10) Zhou C, Zhang S, Zhao M, Wang L, Chen J, Liu B. Investigating the dynamicity of sentiment predictors in urban green spaces: A machine learning-based approach. *Urban For Urban Green*. 2023;89:128130. https://doi.org/10.1016/j.ufug.2023.128130.
11) Gulati K, Kumar SS, Boddu RSK, Sarvakar K, Sharma DK, Nomani MZM. Comparative analysis of machine learning-based classification models using sentiment classification of tweets related to COVID-19 pandemic. *Mater Today Proc*. 2022;51:38–41. https://doi.org/10.1016/j.matpr.2021.04.364.
12) Wang J, Si C, Wang Z, Fu Q. A New Industrial Intrusion Detection Method Based on CNN-BiLSTM. *Computers, Materials and Continua*. 2024;79(3):4297–4318. https://doi.org/10.32604/cmc.2024.050223.
13) Li C, et al. CNN-Transformers for mineral prospectivity mapping in the Maodeng–Baiyinchagan area, Southern Great Xing'an Range. *Ore Geol Rev*. 2024;167:106007. https://doi.org/10.1016/j.oregeorev.2024.106007.
14) Cheker Z, et al. Comparative analysis of VEP signals discrimination methods based on time-frequency transformation and CNN-2D. *Biomedical Engineering Advances*. 2024;7:100114. https://doi.org/10.1016/j.bea.2024.100114.
15) Alzubaidi A, et al. Medical image classification using deep learning and self-supervised learning. *Heliyon*. 2024;10(2):e38997. https://doi.org/10.1016/j.heliyon.2024.e38997.
16) Roy S, et al. Transfer Learning-Enabled Brain Tumor Classification Using Deep CNN with Feature Fusion. In: 2023 International Conference on Computer, Communication, and Informatics Technology (ICCIT). 2023;p. 1–6. https://doi.org/10.1109/ICCIT60459.2023.10441087.
17) Mishra P, et al. Enhanced Adaptive Brain Tumor Detection using Hybrid Deep Ensemble Model;vol. 1785. Singapore. Springer. 2024. https://doi.org/10.1007/978-981-99-8937-9_32.
18) Sharma R, et al. AI-Based Multi-Class Tumor Detection Using Transfer Learning and CNN;vol. 1024. Singapore. Springer. 2024. https://doi.org/10.1007/978-981-97-3562-4_44.
19) Singh NJ, et al. Multimodal Brain Tumor Classification Using Deep CNN and Spatial Context Learning. In: 2023 International Conference on ICT for Sustainable Development (ICICT4SD). 2023;p. 1–6. https://doi.org/10.1109/ICICT4SD59951.2023.10303319.
20) Rathod KG, et al. Brain Tumor Classification Using Deep Transfer Learning with Optimization Techniques. In: 2023 International Conference on Computer, Communication, and Informatics Technology (ICCIT). 2023;p. 1–7. https://doi.org/10.1109/ICCIT60459.2023.10441650.
21) Tiwari RG, Misra A, Maheshwari S, Gautam V, Sharma P, Trivedi NK. Adaptive neuro-FUZZY inference system-fusion-deep belief network for brain tumor detection using MRI images with feature extraction. *Biomed Signal Process Control*. 2025;103:107387. https://doi.org/10.1016/j.bspc.2024.107387.
22) Rahman T, Islam MS. MRI brain tumor detection and classification using parallel deep convolutional neural networks. *Measurement: Sensors*. 2023;26:100694. https://doi.org/10.1016/j.measen.2023.100694.
23) Khan MSI, et al. Accurate brain tumor detection using deep convolutional neural network. *Comput Struct Biotechnol J*. 2022;20:4733–4745. https://doi.org/10.1016/j.csbj.2022.08.039.